
Article:
Evans, M., Skipper, W.A., Buckley-Johnstone, L. et al. (3 more authors) (2021) The development of a high pressure torsion test methodology for simulating wheel/rail contacts. Tribology International, 156. 106842. ISSN 0301-679X

https://doi.org/10.1016/j.triboint.2020.106842

The Development of a High Pressure Torsion Test Methodology for Simulating Wheel/Rail Contacts

M. Evans[1], W.A. Skipper[2]*, L. Buckley-Johnstone[1], A. Meierhofer[3], K. Six[3], R. Lewis[1, 2]

*waskipper1@sheffield.ac.uk

[1]Leonardo Centre for Tribology, The University of Sheffield, Sheffield, United Kingdom

[2]Centre for Doctoral Training in Integrated Tribology, The University of Sheffield, Sheffield, United Kingdom

[3]Virtual Vehicle Research GmbH, Graz, Austria

ABSTRACT

Simulating the wheel/rail contact of a train is traditionally conducted using small-scale twin-disc testing. Here an emerging alternative method, the "high pressure torsion" (HPT) test is introduced. This has advantages over twin-disc testing as only one cycle is used and it is easier to control third body layers during testing. Shear stress data generated is useful on its own, but can also be used to parameterise analytical prediction tools such as the extended creep force model (ECF), which produces creep-force curves from HPT data. This can then be validated against field data to develop a full-scale predictive capability. A detailed account of the HPT methodology development and the procedures for running a typical test are presented along with case studies that illustrate the typical output of HPT testing.

1 INTRODUCTION

Small scale simulations of the wheel/rail contact have historically been focussed on twin-disc testing [1]–[8]. The advantage of twin-disc testing over field testing is the lower associated costs and better control of variables (weather conditions, third body application, etc.). However, the smaller contact area of the twin-disc set-up compared to actual wheel/rail contacts and the constant recycling of the same material over many cycles led to questions over the relevance of the data generated when using it to predict full-scale behaviour. Testing the impact of granular third body materials (e.g. sand) on the contact is a particular problem with small discs being used. It has been found that the impact can be overstated due to: the discs artificially recycling the granular material creating a layer of sand and/or mixing with wear debris to form a third body layer [1], [8]; and the different contact geometry between discs, such as the different angle between discs and the smaller contact area [7], when

compared to the wheel and rail. In addition, it is harder to control the amount of material getting into the contact.

A different test method for assessing friction in the wheel/rail interface, that solves some of the problems associated with twin-disc testing and also works better for third-body materials (especially granular materials), is the high pressure torsion (HPT) method. HPT rigs have traditionally been used to test the effects of high strain rates on materials [9]–[12].

In this paper, the HPT rig is adapted to be a means of assessing the frictional characteristics in the interface between two materials. The procedure also allows the assessment of third body materials in the contact. Buckley-Johnstone et al. [13] have previously presented a paper which utilised the HPT method, however, a number of issues over rig control and running in emerged that steered the need for this paper to highlight: how the issues can be overcome and, an HPT test designed to assess a range of conditions.

HPT testing can also be used to parameterise analytical prediction tools such as the extended creep force (ECF) model first proposed by Meierhofer [14]. The core of the model was the assumption that there exists a third body layer between wheel and rail modelled as a homogeneous and isotropic layer with temperature and normal pressure dependent elasto-plastic behaviour. Once the model is tuned it can be set-up to run for full-scale contacts and validated against field measurements of friction in the wheel/rail interface, thus creating an improved link between small-scale test data and full-scale behaviour.

The aim of the work presented in this paper was to develop an optimised approach for carrying out the HPT tests. This was achieved via developing: a suitable specimen design; application methods for third body layers; ideal rig operation and tuning; data capture and analysis; and interpreting results through linking to creep-force models. The study built on initial HPT pilot studies carried out by Meierhofer [14], Buckley-Johnstone et al. [15], and Skipper et al. [16].

2 HPT CONCEPT

The HPT method is a means of assessing the frictional characteristics between two materials, the procedure also allows the assessment of third body materials in the contact. The principle behind the method is to bring two specimens together to create an annulus (ring) contact, compress them to a set normal pressure and rotate them at a low velocity whilst measuring the torque required to sustain the rotation.

This allows the calculation of shear stresses in the interface and therefore enables characterisation of the friction as the specimens are rotated from the neutral position. Initially, the interface deforms in an elastic manner, but as the test progresses, parts of the contact start to deform plastically until full sliding is achieved. The specimens are made from

wheel and rail material and third body layers can be introduced between the specimens. The principles behind the HPT machine are illustrated in Figure 1.

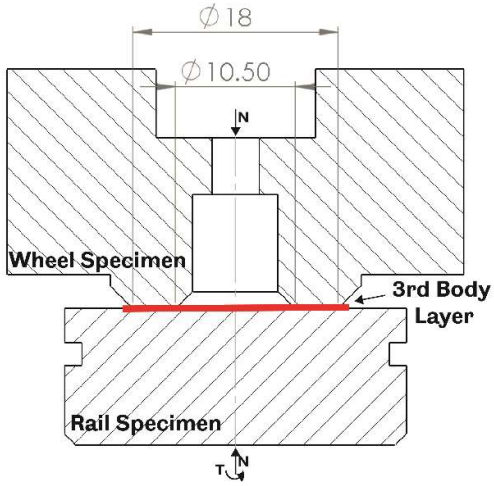

Figure 1- Schematic of HPT Set-up.

The output of a typical HPT test over one cycle (small rotation) is included in Figure 2, which shows how the measured coefficient of traction changes as the specimens rotate. Here the coefficient of traction is defined as the ratio between shear stress and normal pressure in the contact. There are two distinct regions: an “elastic” region (ER); and a “pseudo-plastic” region (PPR). The elastic region is characterised by a steep linear increase in the coefficient of traction over a relatively small displacement. The pseudo-plastic region begins after the linear region has ended. In this region, plasticity effects occur on an asperity level, thereby introducing work hardening effects (in the order of microns) referred to as “local” or “tribological” plasticity, by Six et al. [17]. Due to this phenomenon the coefficient of traction keeps increasing in this region. This type of plasticity should not be confused with plastic deformations seen in deeper regions of the bulk material (in the order of millimetres), called “global” plasticity [17]. This type of plasticity may occur during the first few load cycles until reaching the shake down limit, as is shown later.

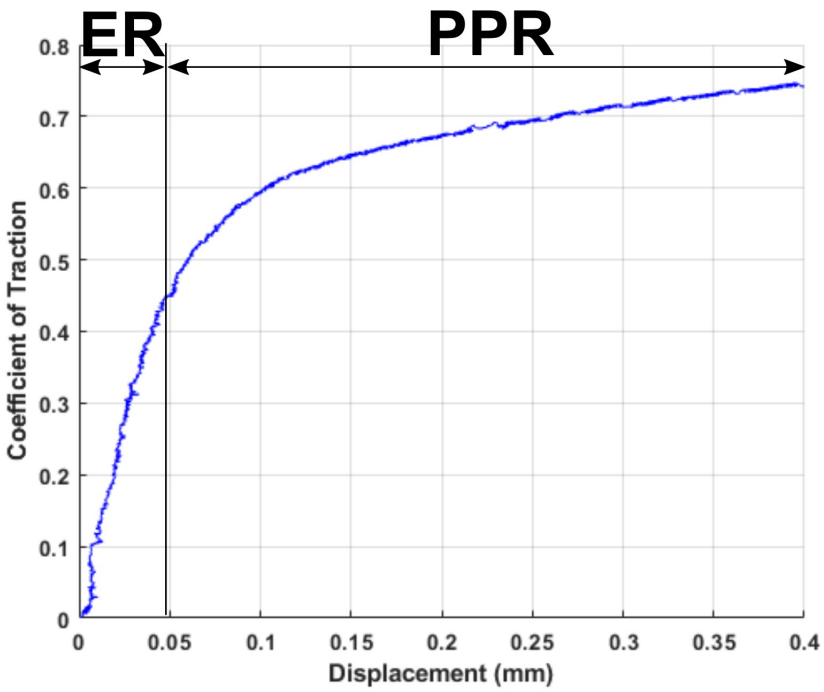

Figure 2- Example of HPT Output.

3 TEST APPARATUS

A servo-hydraulic machine, needed for this type of test, consists of hydraulic actuators operated by electrohydraulic servo valves. Servo-hydraulic systems are often used for precise, high-speed control of high loads, fatigue testing for example. The rig that is used in the development of the HPT method presented in this paper is capable of tension/compression and/or torsion; a schematic of the rig is included in Figure 3.

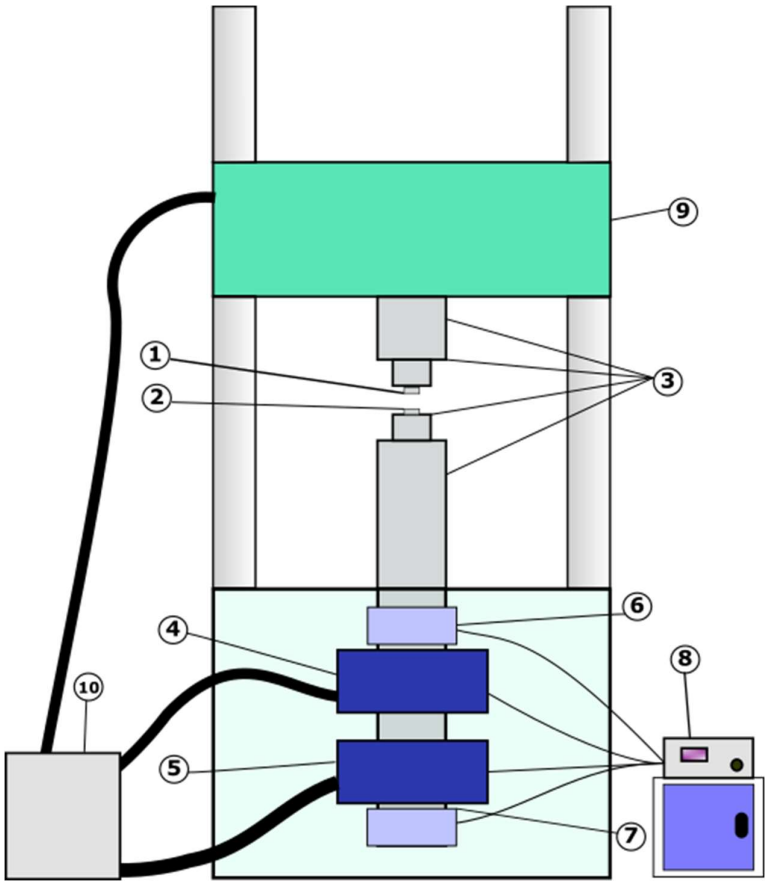

Figure 3- Schematic of HPT Rig.

In Figure 3 the wheel and rail specimens (1 & 2 respectively) are fixed into specimen holders (3). Initially, the specimens are out of contact, but are brought together during testing (see Figure 1 for close-up) and a normal pressure is applied using the axial hydraulic actuator (5). The specimen faces are rotated against each other using a rotational hydraulic actuator (4). The actuators are pressurised using a hydraulic ring main (10) where hydraulic fluid pressurised to around 250 bar; the flow of fluid through the hydraulic actuators is controlled by the servo valves, based on a control signal from an electrical control unit (8). The control unit receives measurements of axial actuator displacements and loads from an LVDT and a load cell (combined into 7). The control unit receives measurements of rotational actuator displacements and loads from an RVDT and a load cell (combined into 6). The control unit has two channels which permit the control of test specimens in both axial and torsional directions. A hydraulically actuated cross-head (9) allows the test rig to accept test apparatus of between around 500mm and 2000mm length.

The average normal stresses in the interface are calculated using the area of the contact patch. For the purpose of the HPT test, the normal stress is assumed to be uniform across the contact patch, ignoring increased pressures at the edges.

The operating capabilities of the machine are shown in Table 1. It should be noted that servo-hydraulic rigs with different capacities are still viable for use with the HPT methodology described in this paper, though different specimen designs will be needed in this case. The specimen design process is included in Section 4.

Table 1- Rated Limits of HPT Servo-Hydraulic Test Machine.

Parameter	Rating
Axial Load Tension/Compression (kN)	±400
Axial Displacement (mm)	±25
Torque (Nm)	±1000
Torsional Displacement (°)	±40
Specimen Length Range (mm)	500-2000

4 SPECIMEN DESIGN

The following section details the geometry selection process involved in designing the contact interface. An annular contact was used with this rig to allow representative contact pressures to be achieved with the load capacity of the machine. Specimens should be freshly ground, flat, and parallel to ensure even pressure around a respective radius of the annular contact. The focus of this section does not include wider design choices and only discusses the design of the contact faces.

4.1 Determination of Creep Stress

Creep stresses are assumed to be uniform across the contact patch, however, at higher radii, the same creep stress will have a greater contribution to the torque supported; therefore, the midpoint radius cannot be used to calculate the creep stress from the measured torque. A value known as the 'effective radius of friction' (ERF) has been used instead as the point at which creep stress is to be calculated. This value is a concept commonly used in clutch design in a machine design [18]. The effective radius of friction is calculated by:

$$ERF = \frac{2}{3}\frac{(R_o^3 - R_i^3)}{(R_o^2 - R_i^2)}$$

Equation 1

where R_o is the outer radius of the contact and R_i is the inner radius of contact.

Until the contact reaches full sliding, the elements at higher radii will have displaced further and therefore be more highly stressed than those at lower radii; for this reason, only an average creep stress can be calculated from the measured torque.

4.2 Specification of Contact Dimensions

Assuming a maximum normal pressure requirement of 1000 MPa (typical value for a wheel tread/rail head contact [19]), and a creep stress not exceeding 700MPa (based on a coefficient of friction of 0.7), the specimen dimensions were calculated to utilise 85% of the capacity of the servo-hydraulic rig; the final 15% is left as a margin for error.

An iterative selection process, through carrying out pilot tests was used to find a balance between minimising the difference in sliding distance between inner and outer radii and reducing edge effects. This resulted in the selection of a contact ring with 10.5 mm and 18 mm inner and outer diameters respectively, as shown in Figure 4. Contact dimensions and predicted maximum forces/torques are shown in Table 2.

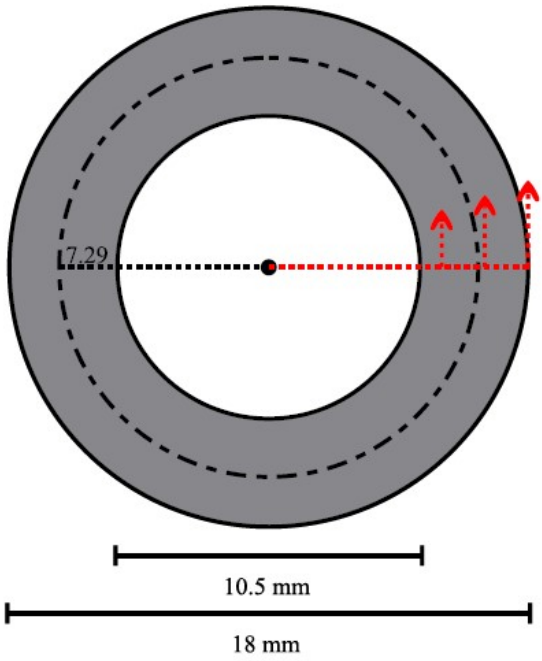

Figure 4- Dimensions of the HPT Contact Area.

Table 2- Contact Dimensions and Predicted Force Requirements.

Parameter	Value
Inner Radius (mm)	5.25
Outer Radius (mm)	9
Effective Radius of Friction (mm)	7.29
Contact Area (mm^2)	169
Maximum Normal Load (@1000MPa Normal Pressure) (kN)	168
Maximum Torque (Assuming 700 MPa Shear Stress) (Nm)	840

5 METHODOLOGY DEVELOPMENT

The design process for developing the HPT methodology was iterative in nature. The following section details some parts of the process, a more thorough overview of the different aspects investigated are detailed elsewhere [20]. This section consists of the initial tests performed on the HPT rig, which are analysed. From this analysis, the following sections detail solutions to any issues encountered, including: developing a run-in procedure; overcoming stick-slip behaviour; and optimising test parameters. Lastly, a check of the repeatability of the method will be presented.

5.1 Initial Test Runs

Figure ***5*** shows the results of preliminary tests performed at three different normal pressures (1000, 750 and 500 MPa). Resulting coefficients of traction (at the end of the cycle) vary between 0.3-0.4; 0.4-0.44 and 0.39-0.45 respectively for normal stresses of 500, 750 and 1000MPa respectively. These are in line with full-scale values [21]. For each contact pressure tested the creep force increases for repeat tests. This set of results also highlight the ’double plateau’ phenomenon.

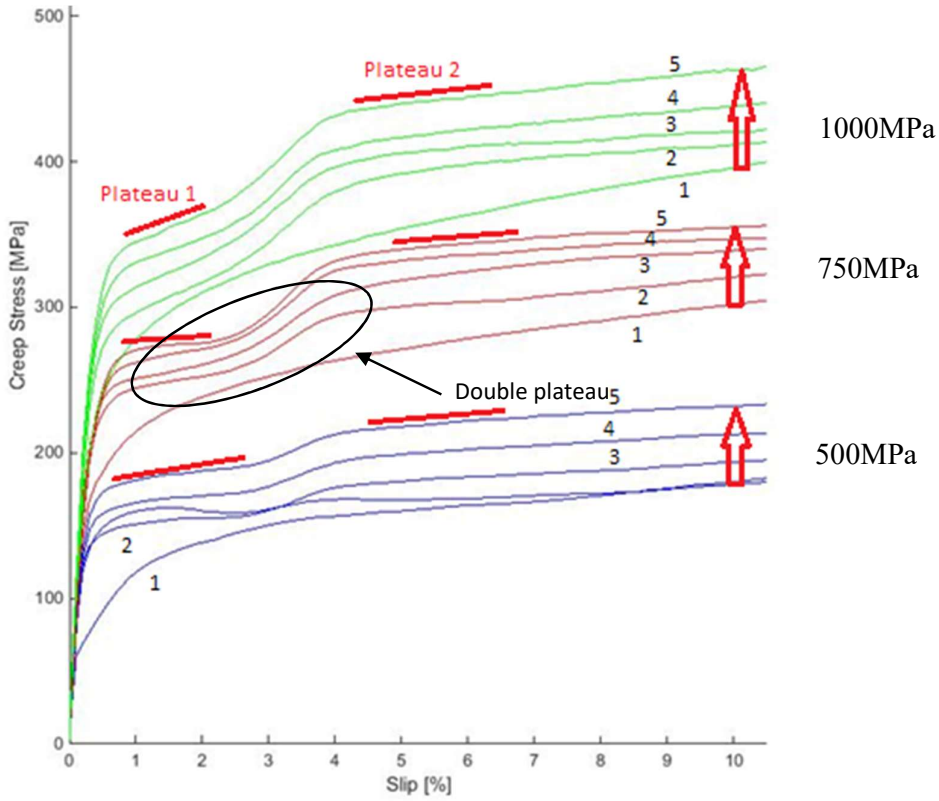

Figure** 5- **HPT test results at three different test pressures.

5.2 Development of a Run-in Procedure

The results shown in Figure ***5*** show that the results from the first runs (lowest creep stresses for each set) tend to have a rounder shape than subsequent tests. They also show that each subsequent test run has higher creep stresses than the previous test result. An explanation for this phenomenon may be the strain hardening of the materials; as the material is plastically deformed, the hardness and yield stress of the material increases. To remove the effects of strain hardening on test results a run-in procedure was developed.

As seen in Section 5.1, an issue that arose from the initial test runs was that the wheel-rail material work hardens as tests progress increasing the shear stress sustained in the contact and eventually causing the surface to break down resulting in shear stresses becoming lower again.

In the real wheel-rail interface both wheel and rail surfaces are work hardened by running along the track and by the passage of vehicles respectively, this process is known as shakedown. To replicate this a run-in procedure of torque oscillations was developed. An example of a single oscillation is shown in Figure 6, where torque is applied in one direction then in the opposite direction.

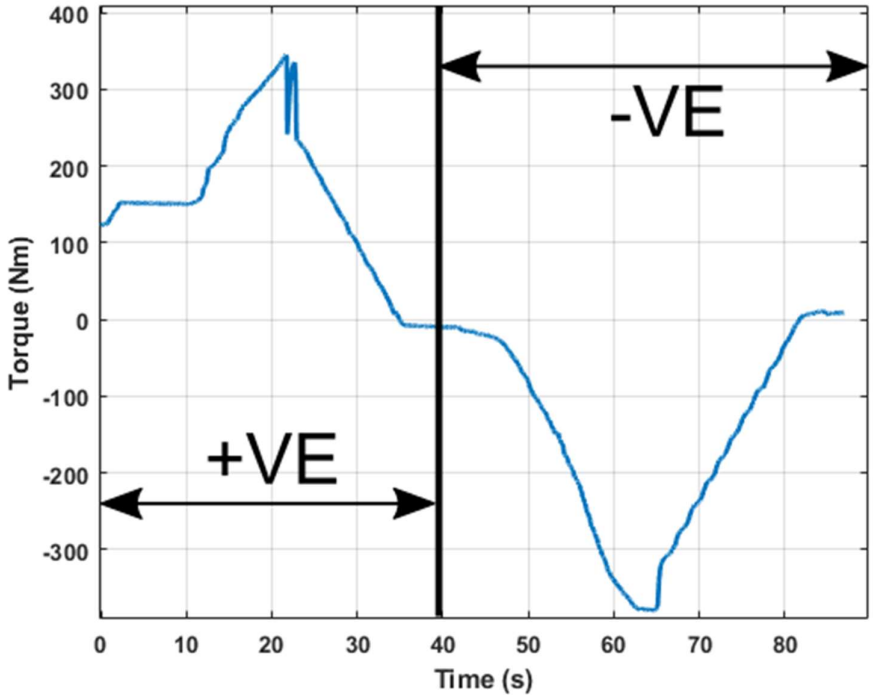

Figure 6- Example of a Torque Oscillation used in the Run-in Procedure.

The aim of the run-in torque oscillations is to work harden the surface of the test specimens with minimal damage to the surface to leave "steady-state" conditions for the actual test. To achieve this, it is necessary to repeatedly load the specimens until plastic deformation (sliding) occurs, whilst limiting the amount of sliding to prevent excessive damage to the surfaces of the specimens.

The torque oscillation procedure was developed to apply torque to the specimens until one of three end conditions is met, at which point the load is released:

1. A specified oscillation torque is met;
2. A specified oscillation distance is met (at the effective radius of friction);
3. A slippage event is detected in the contact (this indicates the limiting friction has been reached, the oscillation is halted to minimise damage to specimens).

Torque oscillations also mitigate alignment issues between the specimens, and therefore should be performed at three separate angular positions; first in the centre of the test rigs positional range, and then at either extreme.

If third bodies are to be applied to a test specimen, the run-in torque oscillations should be performed prior to third body application.

5.3 Test Progression & Limit

The initial test methodology compressed the interface to the required normal pressure, and then rotated the specimen by the required displacement (usually around 12 degrees). To perform subsequent tests, the interface was separated and then rotated back to two thirds the displacement of the previous run and the process was repeated. These initial tests produced results featuring a "double plateau" in the creep stress plot of subsequent runs; this is shown in Figure ***5*** (first run appears lowest in each set).

This double plateau phenomena was initially attributed to the axial misalignment of the specimens. Further experimentation revealed that the double plateau phenomena did not occur if the displacement was advanced between tests, rather than local areas of contact revisiting material that had already been passed over. The two test progression methodologies are illustrated in Figure 77.

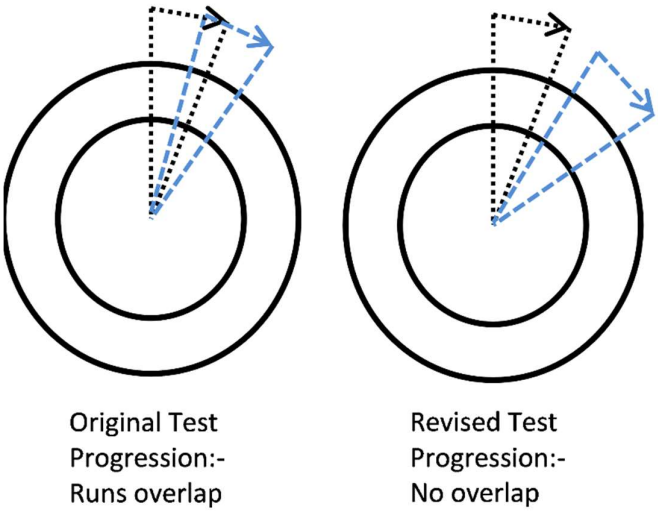

Figure 7- Test Progression.

Tests performed with the revised test progression, did not exhibit the double plateau behaviour seen previously.

Whilst not obvious from data shown in Figure ***5***, eventually, once the test has been run on the same set of specimen multiple times, the specimen surfaces start to break up, and the wear debris acts to reduce the shear stresses supported between the specimens by providing loose particles that ease relative movement. An example of the surface breakdown at the end of the test is included in **Error! Reference source not found.**8.

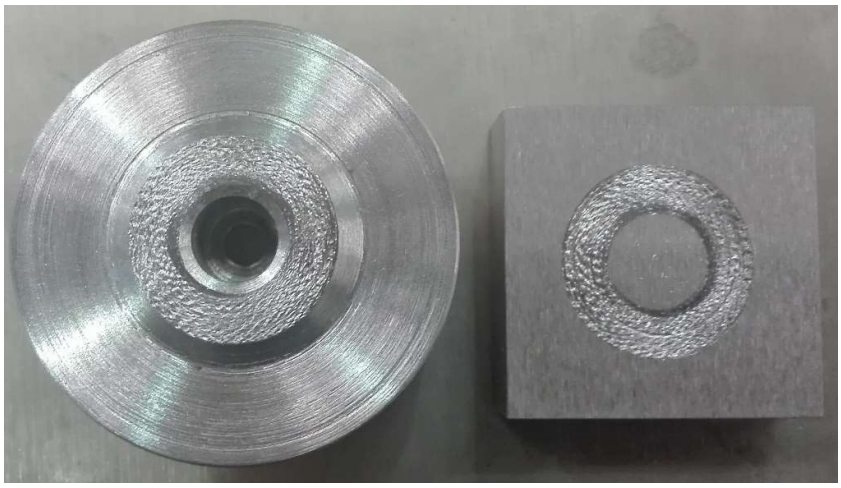

Figure 8- Test Surface Breakdown.

Using the revised test progression, the maximum amount of test runs that could be performed within the rotational range of the rig was 6 sweeps for each pair of specimens. The surface breakdown of the specimens did not have an effect after six tests therefore it does not present a problem in this test methodology, though for other rigs a maximum number of test runs per specimen would have to be established.

5.4 Overcoming Stick-slip Behaviour

During many tests, once the majority of the contact has reached a limiting creep stress, the interface suddenly slips releasing some of the elastic energy built up; the release of elastic energy decreases the creep stress required to stop the slippage and the process repeats. This phenomenon has been noted as stick-slip behaviour, an example of its effects on test data is shown in Figure 9(a).

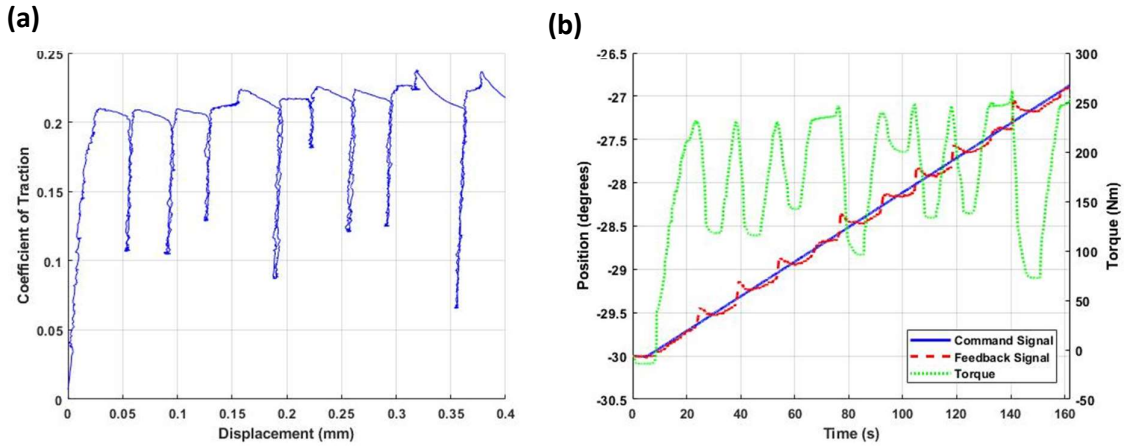

Figure 9- Example of a High Pressure Torsion test exhibiting Stick-Slip Behaviour; (a) The effect of Stick-slip Behaviour on Test Results, (b) A Demonstration of the change in Torque in relation to the Error between the Command and Feedback Signals.

The stick-slip behaviour is feature of the tribological system rather than a problem with the control of the test, however, the control system's response to a slippage event can cause issues. When a slippage event occurs the feedback signal rapidly approaches the command signal of the PID loop, often (especially in a highly tuned system) the feedback exceeds the command signal; this change in error between command and feedback results in the control system reducing, or even reversing the torque applied to the specimens. This reduction in torque means the test does not produce a smooth curve showing elastic deformation followed by sliding as desired, but repeated drops in torque and elastic deformation. An example of this is shown in Figure 9(b).

This issue requires a change in the test parameters being used, therefore some methods for reducing the stick-slip phenomena are included in Section 5.5.3.

5.5 Optimising Test Parameters

5.5.1 Test Sweep Length

A set of tests were performed to determine a suitable sweep length (as measured at the 'effective radius of friction'). Factors considered were:

- Minimisation of sweep length to minimise damage to specimens from excessive sliding;
- Ensuring the sweep length is sufficient for obtaining the full friction behaviour for use in the ECF model.

Figure 10 shows the results from the investigation into test sweep length using clean, dry specimens; it was concluded that a test sweep length of 0.4mm was enough to be confident that the whole interface had entered the sliding regime, whilst minimising damage to specimens.

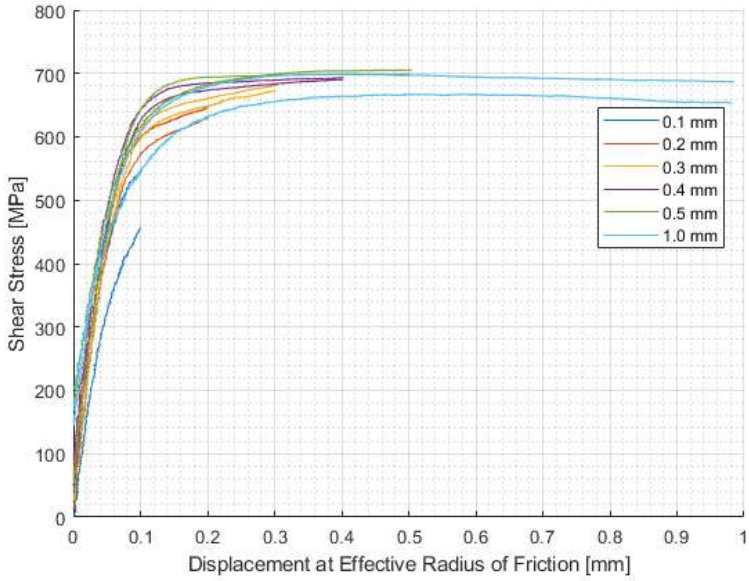

Figure 10- Test Sweep Investigation.

5.5.2 Rotational Sweep Rate

The rotational sweep rate of the HPT test affects the results in a number of ways. Most obviously, the lower the sweep rate, the longer a test sweep takes to complete; this is the only known disadvantage of lowering the sweep rate, assuming the test is running quickly enough that the third body layers do not naturally change over time. However, going too fast could lead to a temperature rise as the frictional heat does not have time to dissipate and data sampling rates may not be high enough to capture sufficient information from the test. A compromise has to be found based on the capabilities of the test-rig and the samples being tested.

5.5.3 Control System Tuning

5.5.3.1 Without Stick-Slip Issues

The tuning of the control system has an important influence on the behaviour of the HPT test. If stick-slip is not a problem, then it is best to tune for the optimum response to the command signal from the controller. Tuned too highly and the actuators will not remain stable, especially when the specimens are out of contact. Tuned too slowly and the system will not be able to follow the control command value. This issue was first noted when assessing the effect of sweep velocity; tests were performed at three different velocities, 0.02, 0.2 and 1 deg/s, the results of this are shown in Figure 11.

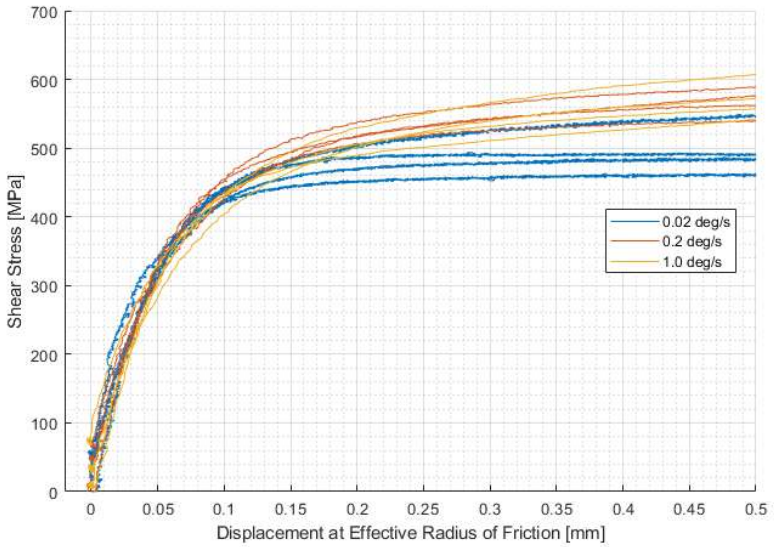

Figure 11- High Pressure Torsion at Three Different Velocities: 0.02, 0.2, 0.1 deg/s.

Figure 11 shows results of HPT tests at multiple velocities. It can clearly be seen that for the lowest speed test (0.02 deg/s), the friction remains reasonably stable once sliding has commenced. This contrasts with the results of the 0.2 and 1 deg/s test, which both show the creep stress rising as sliding progresses.

Figure 12 displays the command following ability of the HPT torsion test for two different speeds, 0.02 and 1 deg/s. The blue lines show the command signals requested by the test controller to perform the test sweep, red lines show the actual position feedback received by the controller. For the 0.02 deg/s case, it can be seen that apart from a small initial deviation, the feedback follows the command almost perfectly. This contrasts with the 1 deg/s case, which shows the feedback lagging significantly behind the command signal; this shows that the PID loop does not effectively follow the command with the test running at this higher speed. To compensate, the Integral portion of the PID loop increases the torque to try and catch up with the command signal, resulting in the rise in torque exhibited in Figure 11. The solutions to this issue include lowering the commanded sweep rate, retuning the PID loops to handle the higher sweep rate or using a very low integral value in the PID loop.

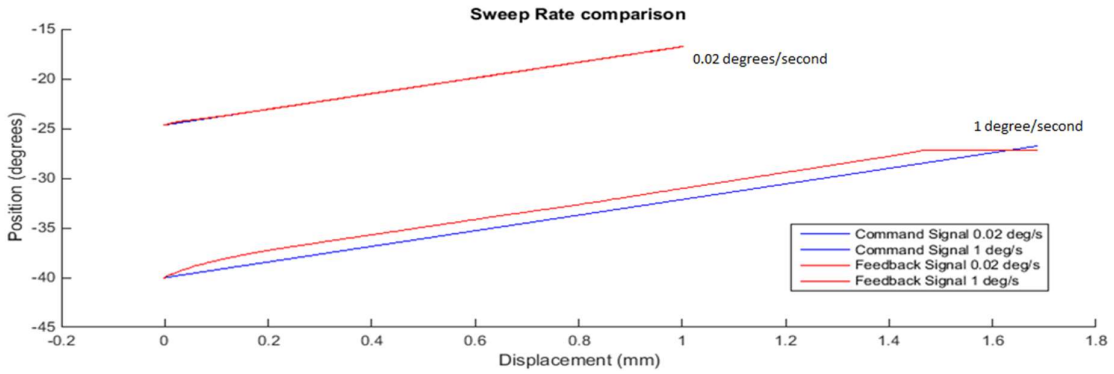

Figure 12- Command Following of the HPT Test at Two Different Velocities.

4.4.2.2 Control System Tuning to Minimise Stick-Slip Disruption

After significant experimentation it was found that the influence of stick-slip behaviour could be minimised by setting the proportional and derivative gains in the PID loop to zero, and using a very low integral gain.

Effectively, the zeroed derivative gain allows the control system to ignore the rapid rate of change occurring during the slippage, and the zeroed proportional gain means the sudden change in errors is not instantly compensated for. Using only the integral gain means the error has to 'build up' to result in a change in behaviour, introducing lag into the response to a rapid change such as a slippage event. Using a very low integral value means that the feedback lags so far behind the command signal that the system barely tries to 'catch up', minimising the increase in torque during the sliding part of the test (see Figure 11); in fact the sweep rate set for the test does not really influence the actual sweep rate achieved. An example of conservatively tuned stick-slip response is shown in Figure 13.

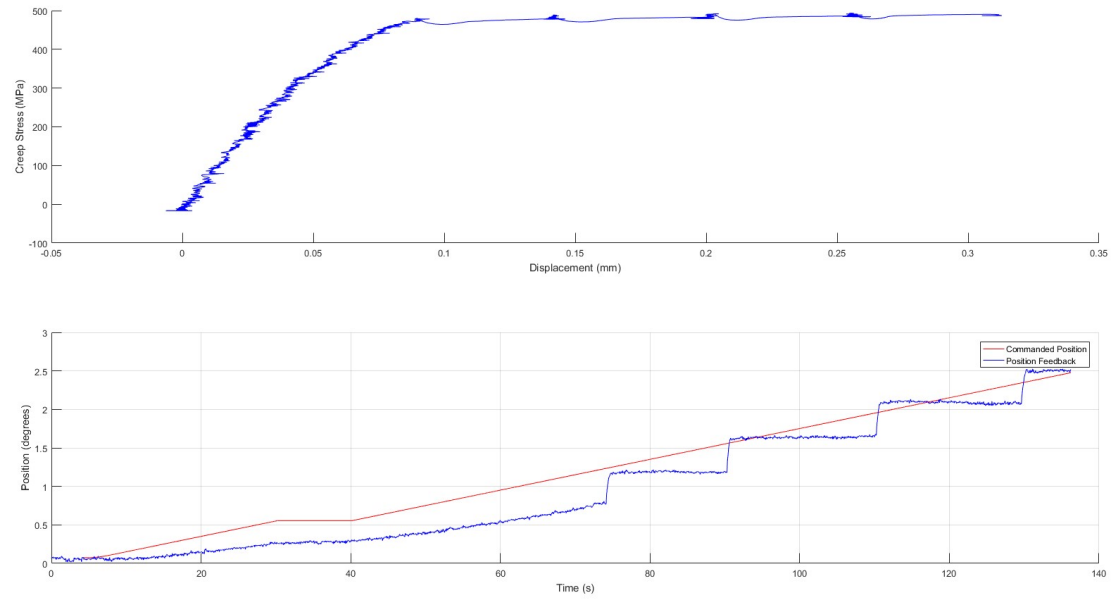

Figure 13- Conservative tuning to minimise reaction to stick-slip behaviour.

Down-tuning the control loop does have consequences as discussed earlier in this section:

- Inaccurate control of sweep rate; thought to be less critical than clean results.
- Rise in torque as result of the integral portion of the PID loop; use a very low 'Integral Gain' value to overcome.

5.6 Repeatability

During testing, the environmental conditions that the tests were conducted under were recorded. Figure 14 shows many different test runs on different test specimens on different days; on all but one occasion the "elastic" region of each curve ends between coefficients of traction between 0.5-0.6 and for all cases the peak coefficient of traction was between 0.65-0.75. These results are repeatable enough for assessing the effect of different contact conditions over repeated tests, even when different ambient conditions are present.

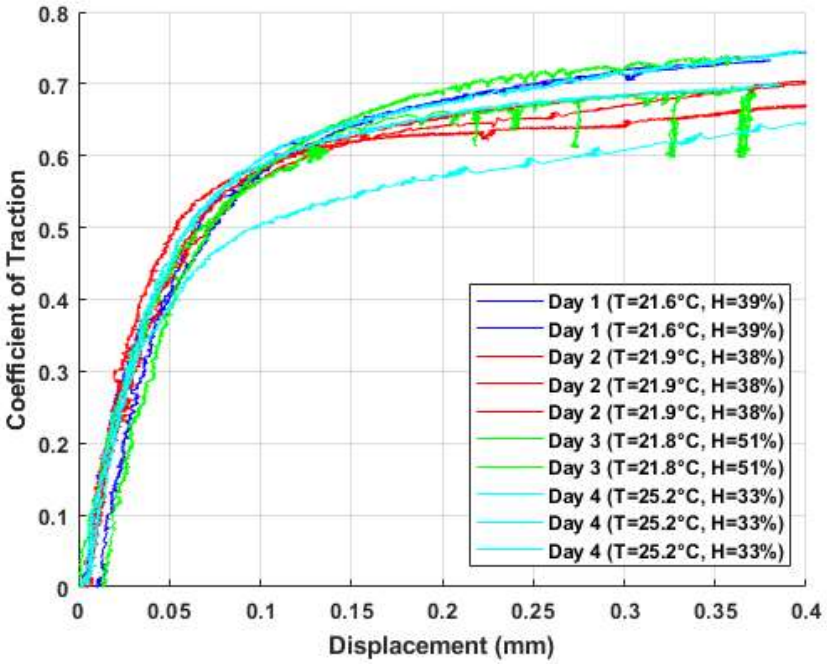

Figure 14- Repeatability of HPT Test over Different Days and Environmental Conditions.

6 TEST SPECIFICATIONS

Section 5 went into the development of the HPT methodology and how issues that arose with the methodology development and rig capabilities were overcome. This section will now go through the current, optimised process of running different tests on the HPT.

6.1 Test Set-up

6.1.1 Specimen Preparation

Specimens are thoroughly cleaned with acetone and paper towels prior to placement in the specimen holders. Care is taken to avoid contaminating specimens following cleaning (including minimising contact with fingers). The specimens are cleaned again following the Specimen Alignment check detailed in Section 6.1.2, since there is no guarantee the pressure sensitive paper is uncontaminated.

6.1.2 Contact Interface Assessment

FUJIFILM Prescale (HHS) Pressure Sensitive Film is used to check the contact interface of the specimens; HHS is the highest pressure rated model of the FUJIFILM Prescale. The parallelism and flatness of the contacting surfaces can be assessed, along with the dimensions of the contact patch. Whilst performing this assessment at testing pressures (up to 900MPa) would be ideal, any possible change in alignment or contact area at higher pressures is deemed insignificant.

The contact interface assessment is performed as follows:

- The pressure sensitive film is compressed between the specimens at three different angular positions, the specifications of the compression are:
    - Angular positions: -40, 0, 40 degrees,
    - Contact pressure, approx.: 150 MPa,
    - Compression time, approx.: 20 seconds,
- Pressure results in a red impression appearing on the Prescale paper, the higher the pressure the darker the colouring,
- Prescale impressions allow assessment of the following:
    - Flatness and parallelism of the specimen interface (even colouring suggests a flat, parallel interface),
    - Measurement of contact patch dimensions,
- Concentric alignment of the interface can also be checked if the specimens are compressed once to leave an indent in the specimen prior to use of Prescale Film.

Once the Interface Assessment has been performed, the measured contact dimensions can be inputted into the test setup script. The specimens should then be cleaned again prior to testing, as detailed in Section **Error! Reference source not found.**.

6.2 Run-in

The run-in procedure for testing is as follows (the values used in a typical test are included in brackets):

1. Specimens are brought into contact at a set normal pressure (900 MPa) at a neutral rotational position (0°),
2. Torque oscillations begin thus (1 cycle):
    a. Specimens are rotated relative to each other until slippage is detected (or a nominal torque or displacement value is met),
    b. Step 2a repeated with the opposite direction of rotation,
3. Torque brought back to zero and specimens brought out of contact,
4. Steps 1 to 3 are repeated at extreme rotational positions (-40° and 40°).

6.3 Test Parameters

Three test sweeps are then performed in either dry conditions or with the requisite third body layer. Test sweep procedure is as follows (the values used in a typical test are included in brackets):

1. Bottom specimen raised till contact is made with the top specimen at required starting angle (-30°, -20°, etc.),
2. Contact pressure increased to required normal pressure (300 MPa, 600 MPa, 900 MPa, etc.),
3. Data logging commences (see Figure 15 for typical recorded dataset),
4. Bottom specimen rotated in the +ve direction through the test sweep length (0.4mm).
5. Once the test has finished, torque is reduced back to zero
6. Bottom specimen lowered,
7. Data logging ends,
8. Test specimens are rotated to required starting angle for next test (as according to section 5.3),
9. Repeat steps 1-7 for required number of runs (3 runs).

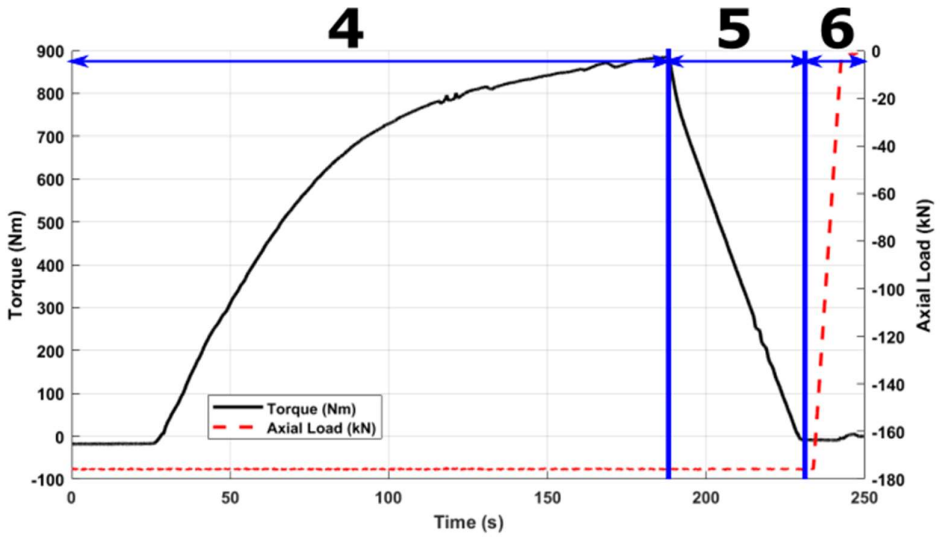

Figure 15- Example of Recorded Data through Steps 4-6.

6.4 Product Application

6.4.1 Liquid Third Body Layers

The requisite amount of liquid (water, oil, grease) is applied via mechanical adjustable volume pipettes. Care must be taken to ensure relatively even coverage throughout the contact. If necessary, a "sweep" can be conducted at very low pressures to ensure even coverage.

6.4.2 Granular Third Body Layers

An amount of particles, representative of field conditions, are placed into the contact with care taken to evenly space the particles, an example of this shown in Figure 16. In this case, the amount of material was calculated to create a particle density of 150 g/m^2 in the contact, the amount currently specified by UK standards as a maximum [22].

Figure 16- Example Particle Placement.

When both particles and liquid are being applied, the particles are placed first according to the aforementioned procedure and liquid is then applied in the same manner as set out in section 6.4.1.

An example of HPT work involving granular third body layers can be found in work by Skipper et al. [16].

6.4.3 Top-of-Rail Products

The amount of top-of-rail product, in this case a water based drying friction modifier, being applied to the contact to create application amounts similar to field testing was very small. Therefore, to ensure the friction modifier is applied evenly the product is to be diluted in water (note that a different approach would be required for a top-of-rail lubricant e.g. oil or grease).

Top-of-rail products are applied to HPT specimens using the following methodology:

1. Friction modifier and distilled water mixed to produce requisite amount of fluid at requisite concentration,
2. Specimens cleaned with acetone prior to friction modifier dilution application,
3. Rubber washers placed on the specimens with a known inner diameter, this provides the known application area,
4. 400 µL of the required friction modifier dilutions/water control placed on each sample, with effort made to ensure the dilution is spread around the application area,
5. Specimens placed in a vacuum oven, to provide slight heat and vacuum to encourage evaporation whilst preventing oxidation,
6. Once all water has evaporated, the specimens are removed from the vacuum oven and carefully stored under dry conditions for testing.

7 ECF MODELLING

Figure 17 summarises the main ideas and the modelling approach of the extended creep force (ECF) model. This model is to predict the creep force characteristic of wheel-rail contacts (see bottom left subplot). This is based on the idea that there always exists a third body layer (3BL) between wheel and rail, which has been confirmed by lab and field experiments (see e.g. top left subplot). Following the ECF modelling approach, the 3BL comprises “real” 3BLs (sand particles, wear debris, iron oxides, etc.) and the near-surface layers of wheel and rail including roughness and the related “tribological” plasticity phenomena [17]. It is assumed that the wheel and the rail behave elastically, while the 3BL is assumed to have an elastic-plastic behaviour (see top centre subplot). To describe this elastic-plastic behaviour of the 3BL, Voce’s hardening law [23] is used, where the model parameters are chosen as contact

pressure and temperature dependency (top right subplot). For parameterisation of the 3BL model the HPT test, as presented in this work, can be used. The temperature dependency of the parameters has been determined by vehicle tests running in the high creepage regime to observe falling friction effects. Finally, the 3BL model has been implemented into a brush model for rolling contacts (bottom right subplot) to predict the creep force characteristic (bottom left subplot). The ECF model is able to describe measured characteristics much better than classical theory e.g. falling friction at high creepages, a gentle transition from a steep linear region to a saturated region, speed and load dependency, etc. A detailed description of the model can be found in [8,11,18].

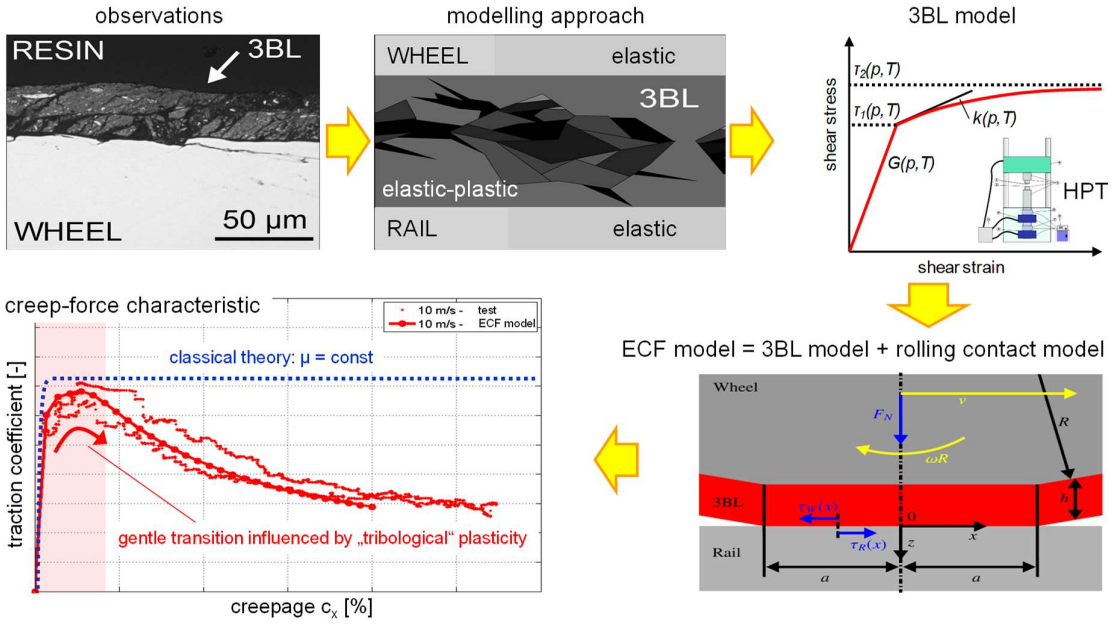

Figure 17- ECF model: approach and methodology.

To summarize, the ECF model in combination with the described methodology for model parameterisation allows for the prediction of the creep force characteristic of rolling contacts, based on “simple” HPT tests carried out in labs. Figure 18 shows an example for dry conditions. In the left subplot, test results from the HPT rig under different contact pressures is depicted. These results have been used to parameterise the 3BL model as part of the ECF model. Results from the 3BL model are also presented in the figure, showing a good agreement with experimental values. In the right subplot, the predicted creep force characteristic for full-scale rig (FSR) conditions is shown. A good agreement between the ECF predictions and the FSR result can be seen. The ECF model accurately predicts that the maximum creep force occurs at a creepage of about 10%, which is much higher than classical theory would predict (< 1%).

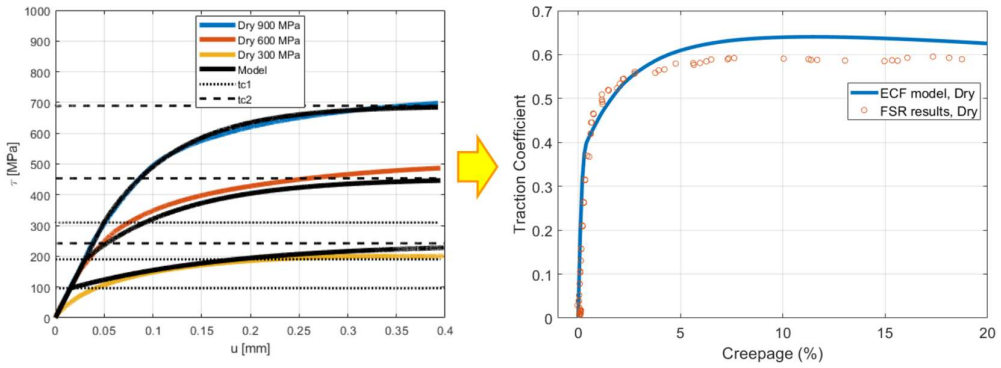

Figure 18- - Test results for dry conditions from HPT test together with results from the 3BL model (left plot) as basis to predict the creep force characteristic of a rolling contact (right plot) [14].

8 CASE STUDIES

The following section outlines three different case studies involving three different types of third body layers. This section should give the reader an idea of what the outputs of the HPT method look like and what can be inferred from these results. In addition to the studies presented here, another study using the HPT methodology has previously been performed [16].

8.1 Dry Contact

Dry baseline tests were performed at a normal pressure of 900, 600 and 300 MPa. The results are shown in Figure 19, presented both in terms of creep stress, and creep stress normalised against normal pressure (traction coefficient). For each normal pressure tested, three runs are shown.

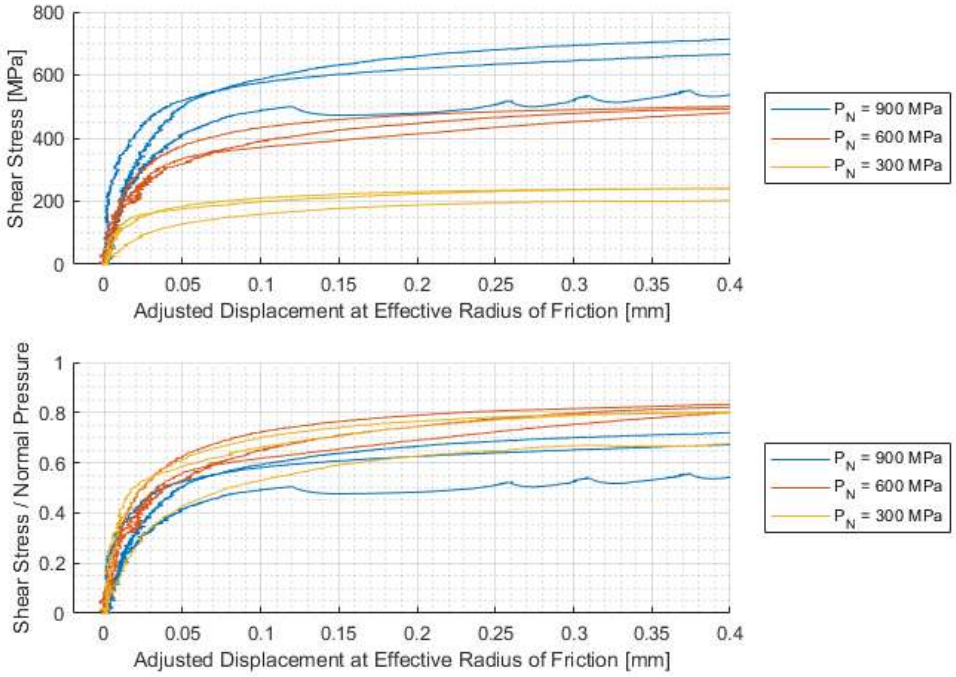

Figure 19- Dry Baseline Tests.

Figure 19 shows dry baseline results from tests performed at normal pressures of 300, 600 and 900 MPa. Results at all three normal pressures exhibit a steep initial elastic region, a transition region, and finally complete sliding.

When normalised against the normal pressure, it can be seen that the 300 and 600 MPa normal pressure results behave similarly, each with a coefficient of traction around 0.8; the 900 MPa normal pressure results reach a slightly lower maximum friction in three runs, but appear to still be work hardening with each test run. This is most likely due to the run-in procedure being performed at 900 MPa normal pressure for all three test pressures. For the 300 and 600 MPa cases, the run-in procedure work hardened the materials to stresses above the stresses experienced during the test, as a result, the test results exhibit a relatively stable friction; for the 900 MPa case, the run-in procedure was performed at the test pressure, and work hardening is still occurring as the test runs progress.

The first run of the 900MPa test set experiences stick-slip oscillations, whilst subsequent runs do not.

Comparing the adhesion coefficients from tests in Figure 19 to previous dry tests conducted on a twin disc set-up [2], [4] shows that the peak adhesion coefficient of between 0.6-0.8 measured using the HPT methodology is similar to that measured on the twin disc set-up (adhesion coefficient ~0.6). In two separate field tests performed by Arias-Cuevas et al. [24] and Six et al. [21]; the adhesion coefficient was measured as 0.2-0.23 and 0.25-0.4 (at slip

rates of 0-10%) respectively. When comparing these field adhesion coefficient measurements to HPT data it can be seen that the HPT adhesion coefficient is significantly higher, possibly due to the thorough cleaning of the contact before testing as well as environmental conditions.

8.2 Friction Modifier

The following case study examines the effects of applying a commercial friction modifier to the HPT interface. This will involve an overview of results obtained from tests with representative amounts of friction modifier and tests with an over-application.

8.2.1 Controlled Dosages

High Pressure Torsion tests were performed with 5 different dosages of dry friction modifier present in the contact, these were performed at 600MPa and are shown compared to a dry baseline in Figure 20.

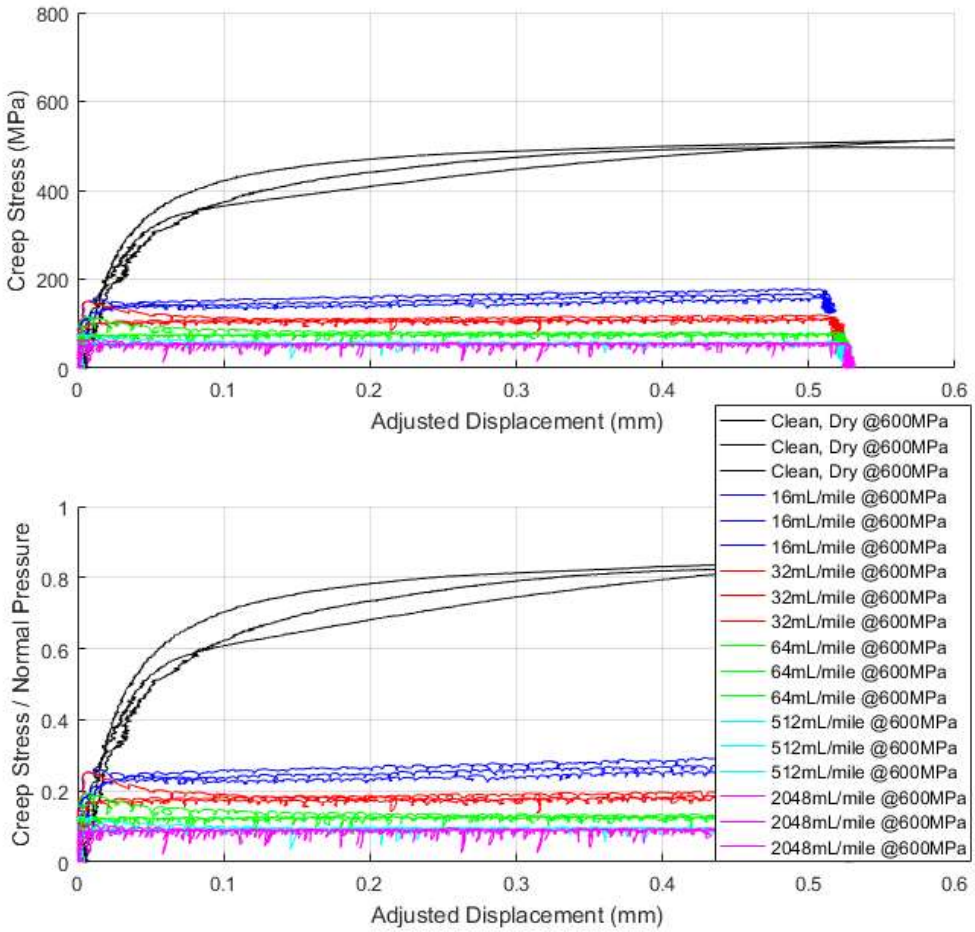

Figure 20- Friction modifier at realistic dosages (compared with a dry baseline).

The results in Figure 20 show that even the lowest dosage of dried friction modifier reduces the coefficient of friction from >0.8, to <0.3, similar values for friction modifiers were found at full scale tests by Buckley-Johnstone et al. [25]. Each increase in the dosage of friction modifier reduced the friction levels further, until a minimum friction of around 0.1 (512 mL/mile) is reached, at which point increasing the friction modifier dosage does not result in a further drop in friction.

It is also notable that the initial gradient of the dry cases is significantly shallower than the friction modifier cases.

8.2.2 Over-applications

High Pressure Torsion tests were also performed with a gross over-application of undiluted friction modifier, both wet, and partially dried; these were performed at 900MPa and are shown compared to a dry baseline in Figure 21.

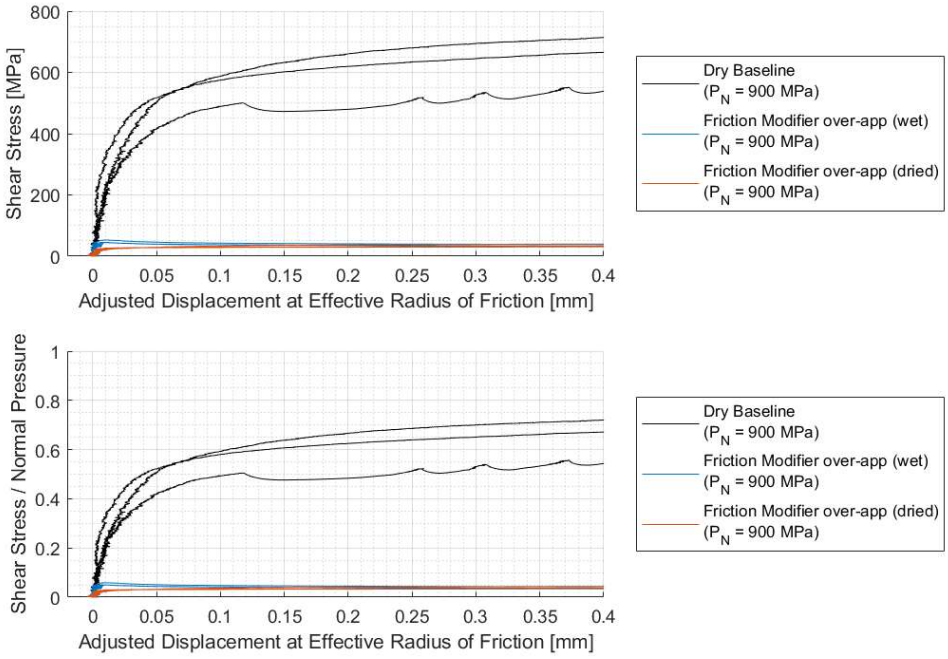

Figure 21- Friction modifier over application (compared with a dry baseline).

Figure 21 shows that an over application drops the coefficient of friction from around 0.7 to below 0.05. Dry product does not increase the coefficient of friction, but it does change the shape of the initial curve; when the material is wet, the coefficient of friction is initially higher until friction levels lower as slippage occurs.

8.3 Low Adhesion

Figure 22 shows the effect adhesion reducing third body layers have on the measured adhesion coefficient. In these tests, the measured adhesion coefficient is markedly reduced by both the presence of 20 µL of water and a sycamore leaf powder wetted with 40 µL of water.

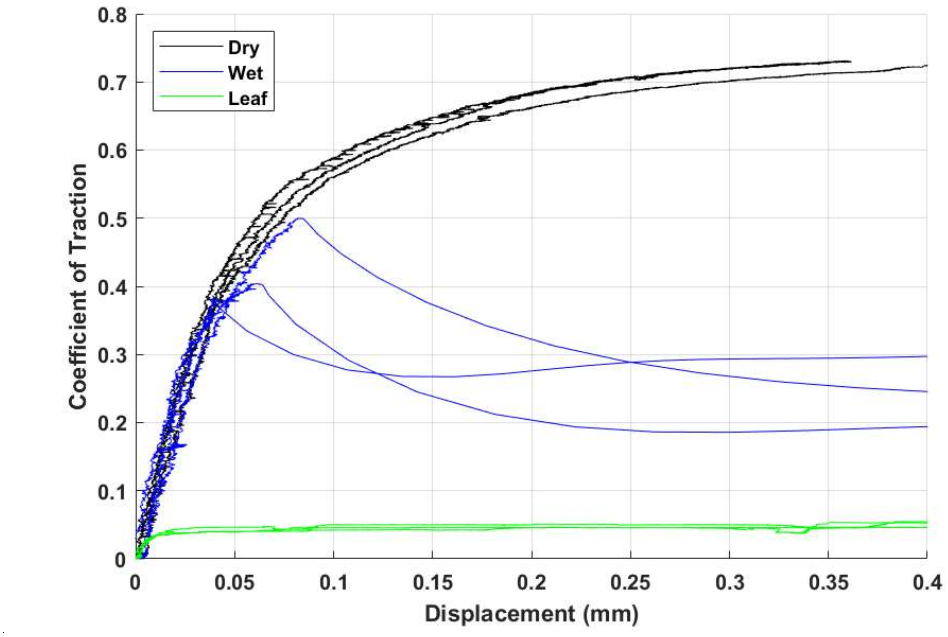

Figure 22- Comparison of Dry Tests with Tests with Adhesion Reducing Third Body Layers.

One notable change between dry and wet tests is the steep reduction in adhesion coefficient after the initial "stiff" elastic section of the curve is completed. This can be attributed to a gross stick-slip event under a PID loop with no proportional element and a very small integral element (see section 5.5.3 for more detail), thereby making the control system very slow to react to this stick-slip event.

9 CONCLUSIONS

A new method for simulating the wheel/rail contact has been introduced, the high pressure torsion (HPT) method. The HPT method has advantages compared to more the typical small-scale twin-disc testing approach, especially when assessing the effect of third body layers on adhesion within the contact. Case studies have been presented that demonstrate the method's efficacy for testing the effect of third body layers within the HPT interface.

The method has been used to parameterise analytical approaches for predicting creep force behaviour, such as the ECF model, which can then be used to assess full-scale behaviour. This

use of the ECF model was considered successful, but has not been included within the scope of this paper; more can be found in the thesis of Evans [20].

Further work will focus on:

- Testing a range of different adhesion materials to assess their effect on the wheel/rail contact;
- Working on methods for reducing the influence of the stick-slip phenomena on test results where low adhesion third body layers are being simulated.

ACKNOWLEDGMENT

The publication was partly written at Virtual Vehicle Research GmbH in Graz, Austria. The authors would like to acknowledge the financial support of the COMET K2 Competence Centers for Excellent Technologies Programme of the Federal Ministry for Transport, Innovation and Technology (bmvit), the Federal Ministry for Digital, Business and Enterprise (bmdw), the Austrian Research Promotion Agency (FFG), the Province of Styria and the Styrian Business Promotion Agency (SFG).

REFERENCES

[1] O. Arias-Cuevas, Z. Li, R. Lewis, and E. a Gallardo-Hernández, "Laboratory investigation of some sanding parameters to improve the adhesion in leaf-contaminated wheel–rail contacts," *J. Rail Rapid Transit*, vol. 224, no. 3, pp. 139–157, 2010.

[2] Z. Li, O. Arias-Cuevas, R. Lewis, and E. A. Gallardo-Hernández, "Rolling–Sliding Laboratory Tests of Friction Modifiers in Leaf Contaminated Wheel–Rail Contacts," *Tribol. Lett.*, vol. 33, no. 2, pp. 97–109, 2009.

[3] O. Arias-Cuevas, Z. Li, R. Lewis, and E. A. Gallardo-Hernández, "Rolling–sliding laboratory tests of friction modifiers in dry and wet wheel–rail contacts," *Wear*, vol. 268, no. 3–4, pp. 543–551, 2009.

[4] O. Arias-Cuevas, Z. Li, and R. Lewis, "A laboratory investigation on the influence of the particle size and slip during sanding on the adhesion and wear in the wheel-rail contact," *Wear*, vol. 271, no. 1–2, pp. 14–24, 2010.

[5] E. A. Gallardo-Hernandez and R. Lewis, "Twin disc assessment of wheel/rail adhesion," *Wear*, vol. 265, no. 9–10, pp. 1309–1316, 2008.

[6] R. Lewis and R. S. Dwyer-Joyce, "Wear at the wheel/rail interface when sanding is used to increase adhesion," *J. Rail Rapid Transit*, vol. 220, no. 1, pp. 29–41, 2006.

[7] R. Lewis, R. S. Dwyer-Joyce, and J. Lewis, "Disc machine study of contact isolation during railway track sanding," *J. Rail Rapid Transit*, vol. 217, no. 1, pp. 11–24, 2003.

[8] A. Meierhofer, C. Hardwick, R. Lewis, K. Six, and P. Dietmaier, "Third body layer-experimental results and a model describing its influence on the traction coefficient," *Wear*, vol. 314, no. 1–2, pp. 148–154, 2014.

[9] K. Edalati and Z. Horita, “A review on high-pressure torsion (HPT) from 1935 to 1988,” *Mater. Sci. Eng. A*, vol. 652, pp. 325–352, 2015.

[10] A. Hohenwarter and R. Pippan, “Sample Size and Strain-Rate-Sensitivity Effects on the Homogeneity of High-Pressure Torsion Deformed Disks,” *Metall. Mater. Trans. A Phys. Metall. Mater. Sci.*, vol. 50, no. 2, pp. 601–608, 2019.

[11] T. Leitner, G. Trummer, R. Pippan, and A. Hohenwarter, “Influence of severe plastic deformation and specimen orientation on the fatigue crack propagation behavior of a pearlitic steel,” *Mater. Sci. Eng. A*, vol. 710, no. October 2017, pp. 260–270, 2018.

[12] R. Pippan, S. Scheriau, A. Hohenwarter, and M. Hafok, “Advantages and Limitations of HPT: A Review,” *Mater. Sci. Forum*, vol. 584–586, no. January, pp. 16–21, 2008.

[13] L. E. Buckley-Johnstone *et al.*, “Assessing the impact of small amounts of water and iron oxides on adhesion in the wheel/rail interface using High Pressure Torsion testing,” *Tribol. Int.*, vol. 135, no. October 2018, pp. 55–64, 2019.

[14] A. Meierhofer, “A New Wheel-Rail Creep Force Model based on Elasto-Plastic Third Body Layers,” TU Graz, 2015.

[15] L. E. Buckley-Johnstone, G. Trummer, P. Voltr, K. Six, and R. Lewis, “Full-scale testing of low adhesion effects with small amounts of water in the wheel/rail interface,” *Tribol. Int.*, 2020.

[16] W. A. Skipper, S. Nadimi, A. Chalisey, and R. Lewis, “Particle Characterisation of Rail Sands for Understanding Tribological Behaviour,” *Wear*, vol. 432–433, no. 202960, 2019.

[17] K. Six *et al.*, “Plasticity in wheel–rail contact and its implications on vehicle–track interaction,” *Proc. Inst. Mech. Eng. Part F J. Rail Rapid Transit*, vol. 231, no. 5, pp. 558–569, 2017.

[18] R. Budynas and J. K. Nisbett, *Shigley’s Mechanical Engineering Design*. 2015.

[19] R. Lewis and U. Olofsson, “Mapping rail wear regimes and transitions,” *Wear*, vol. 257, no. 7–9, pp. 721–729, 2004.

[20] M. D. Evans, “Performance Assessment of Friction Management Products in the Wheel-Rail Interface,” University of Sheffield, 2018.

[21] K. Six, A. Meierhofer, G. Müller, and P. Dietmaier, “Physical processes in wheel–rail contact and its implications on vehicle–track interaction,” *Veh. Syst. Dyn.*, vol. 53, no. 5, pp. 635–650, May 2014.

[22] Rail Safety and Standards Board, “GMRT2461 Sanding Equipment (Issue 2),” 2016. [Online]. Available: https://www.rssb.co.uk/rgs/standards/GMRT2461 Iss 2.pdf.

[23] S. Alexandrov, “A Property of Equations of Rigid/Plastic Material Obeying a Voce-Type Hardening Law,” *Meccanica*, vol. 34, pp. 349–356, 1999.

[24] O. Arias-Cuevas and Z. Li, “Field investigations into the adhesion recovery in leaf-contaminated wheel–rail contacts with locomotive sanders,” *J. Rail Rapid Transit*, vol. 225, no. 5, pp. 443–456, 2011.

[25] L. Buckley-Johnstone, M. Harmon, R. Lewis, C. Hardwick, and R. Stock, “A comparison of friction modifier performance using two laboratory test scales,” *Proc. Inst. Mech.*

Eng. Part F J. Rail Rapid Transit, vol. 233, no. 2, pp. 201–210, 2018.